International Journal of GEOMATE, March, 2020, Vol.18, Issue 67, pp. 63-70
ISSN: 2186-2982 (P), 2186-2990 (O), Japan, DOI: https://doi.org/10.21660/2020.67.5710
Special Issue on Science, Engineering and Environment

AFM VISUALIZATION OF PHYTOPLASMA DNA IMMOBILIZATION AND HYBRIDIZATION EVENT ON CHITOSAN MODIFIED SPCE SURFACE

*Porntip Wongkaew[1] and Buddhapala Wongkaew [2]

[1] Faculty of Agriculture, Khon Kaen University, Thailand; [2]Metropolitan Waterworks Authority, Thailand

*Corresponding Author, Received: 12 June 2019, Revised: 04 Sept. 2019, Accepted: 02 Dec. 2019

ABSTRACT: The evidence of DNA immobilization and hybridization on a functional surface is demonstrated in this presentation following the high-resolution atomic force microscopic (AFM) direct observation. A planar functional surface was fabricated by self-assembly of a biopolymer chitosan onto screen-printed carbon electrode (SPCE) concerning to its excellent covalent bonding binding of biomolecules. The target DNA molecules were extracted from important phytoplasma diseased plants such as sugarcane white leaf (SCWL), burmuda grass white leaf (BGWL) and sesame phyllody (SP). The real image in actual posture of long chain natural DNA and the well-known structure of the DNA double helix were obviously visualized following the DNA immobilization and subsequent transitional hybridization with their complementary DNA. The coordinate quantitative parameters of AFM images such as line profile analysis, surface roughness, power spectrum density (PSD) algorithm and fractal dimension were also determined. The width size of double stranded DNA and the specific hybrid DNA were apparently almost 2 folds bigger than their single stranded DNA. Whereas an aggregation and growth mechanism of those DNAs on chitosan modified SPCE surfaces were mainly stacked in vertical direction and grown beyond a diffusion limited model as indicated by their fractal dimension values around 2 to 3. This phenomenon is hence valuable for the verification and the efficient development of diagnostic DNA-based devices.

Keywords: Atomic force microscope, Chitosan modified SPCE, DNA immobilization and hybridization, Real actual image

1. INTRODUCTION

At present, biosensing technology has perceived a profound attention due to human life necessity for accurate, specific, ultrasensitive and speedy automatic point of care diagnostic tools. Ubiquitous applications including healthcare monitoring of human, animal husbandry, plant production, food and environment security are growing adopted [1], [2], [3], [4]. For decades, researches on coupling biomolecules with electronic detection devices have been pursued for effective sensing application. Several biological elements and molecules such as cells, antibodies, enzymes, receptor proteins, lectins, and nucleic acids are considerately competent. Among these, DNA (Deoxyribonucleic acid) has attracted intensive focus according to its structural versatility and genetic functionality that makes a top capacity for target discrimination. Typically, DNA based biosensing system is manipulated through functional surface sensor containing the selected single stranded DNA molecule attached onto an electroactive transducer. The target detection is subsequently operated on the most selective reactions in nature basis of nucleic acid hybridization that allows several readout strategies such as colorimetry, spectroscopy, electrophoresis and especially the electrochemical signalling [1], [2], [5]. Therefore immobilization and hybridization of the DNA on transducer surface is exactly critical for desirable sensitivity and specificity including overall measurable electronic signal generation of the biosensor.

A direct physical anchor of DNA on the capture molecules at a basal electrode surface is one of the most common immobilization approaches. This procedure involves the simple electrostatic self-assembled layer by layer technique [1], [2], [5]. Selection of a proper working platform is crucial for this type of DNA immobilization and fabrication of the DNA sensor. Among several elements, the carbon made up electrodes are favoured as basal transducers due to their ready available chemical inert material with a high conductivity and low background current that offer a wide range of modification [6], [7], [8]. Stability and sensitivity of the detection performance are also affected by materials chosen to modify the electrode surface for DNA capturing. Besides many synthetic conducting polymers that have been explored for suitable DNA immobilizing support, there is also natural polymer such as chitosan which offer a super functionality with an intrinsically strong affinity to different types of biological molecules. The numerous

hydroxyl and amino groups containing chitosan enable a contribution of both inter and intra-molecular hydrogen bonding interactions for highly stable DNA entrapment on its matrix [2], [5]. Previous studies on the establishment of high conductivity and bioaffinity modified electrodes using the versatile chitosan biomaterial have been sequentially reported [1]-[5], [7], [8]. Both modifications based on glassy carbon (GCE) and screen-printed carbon electrode (SPCE) were proven effective. However, the SPCE becomes the most favourite choice of manipulation due to its facilitation of minimal regulate system, low cost and disposability. Electrochemical potency and morphological properties of the modified SPCE surface with an incorporation of chitosan has been demonstrated via its voltammetric performances and atomic force microscopic (AFM) investigation [4], [7]. The feasibility of chitosan modified carbon electrode for DNA immobilization and plant disease diagnosis by this formulated sensor was also indicated in cases of sugarcane white leaf (SCWL) using both a short sequence of ssDNA probes specific to the causal SCWL-16S rDNA phytoplasma [1], [5], [9] and a long chain genomic ssDNA probe from the SCWL diseased plants [2], [5]. Satisfactory detection capability could be approved through electrochemical voltammetric sensing scheme no matter how short or long ssDNA chain probe is utilized. Preliminary observation of the sensing surfaces by AFM allowed a visual image of the immobilized ssDNA probe on chitosan matrix and the corresponding pairing coupled strands of hybridization occurrence. However, a study in more criteria details both quantitatively and morphologically is still needed to elucidate the reality of hybridization dynamics especially the classical double helix forming postulated by Watson and Crick [10] that no one could actually see it ever.

With reference to those excellent advantages of the chitosan modified electrodes previously reports, this current study was further motivated using three genomic DNA, each, from phytoplasma pathogens that cause important plant diseases in Thailand [11] such as sugarcane (*Saccharum officinarum* L.) white leaf (SCWL), burmuda grass (*Cynodon dactylon* L.) white leaf (BGWL) and sesame (*Sesamum indicum* L.) phyllody (SP) as representative illustrations for a close investigation of the actual hybridization event. The AFM was employed for the intensive speculation due to its superb efficiency in imaging at micro and nanoscale over than other devices at this moment. This microscopy not only offers the capacity to visualize nanometric features in two and three dimensions but also the physicochemical characteristics including its spatial distribution mapping of surfaces at different stages of the molecular assembly. Moreover, observation can be directly performed without any special preparation requirement [3], [4], [7], [8], [12]. In a while, successful direct visual evidence of DNA immobilization and hybridization phenomena could be captured and ascertained by the AFM imaging and corresponding quantitative topographic parameters. The first real image of the being tie in helical posture of the complementary DNA couple during a hybridization event could also be validated in this article.

2. MATERIALS AND METHODS

2.1 Materials

Screen printed carbon electrode (SPCE) model DRP-150 consisting of 4 mm spot carbon as working electrode surrounded with a counter electrode platinum line and a reference electrode silver line was provided by DropSens, S.L. Llanera (Asturias) Spain. Chitosan at 85% degree of deacetylation with a molecular weight of 0.28 kDa was obtained from Bioline Lab, Co., Thailand. Analytical graded chemicals for reagent preparation were purchased from Sigma-Aldrich Co. LLC, USA and Ajax Finechem Pty,Ltd., Australia. High purity deionized water of 18.2 MΩ from Milli-Q RG system (Millipore Corporation, MA, USA) was used in all solutions. The diseased samples, sugarcane white leaf (SCWL) , burmuda grass white leaf (BGWL), and sesame phyllody (SP) from collection maintained in the insect proof disease nursery of Plant Pathology Division of the Faculty of Agriculture, Khon Kaen University, were used for a pure source of each causal phytoplasma DNA extraction . Healthy sugarcane, burmuda grass and sesame maintaining far apart in another insect proof nursery were brought as the challenge controls. Preliminary confirmation for the absence or existence of each causal phytoplasma was done by PCR with a set of specific primer pair of both the 16S rDNA and 16-23S rDNA reported earlier [9].

2.2 Preparation of Chitosan Modified Electrode Platform

Chitosan solution (1%, w/v) was done by dissolving 1 g chitosan in 100mL of 1% (v/v) acetic acid solvent and the solution was filtered to remove insoluble materials. A self-assembled monolayer of chitosan was formed on carbon working spot of screen-printed carbon electrode (SPCE) by applying a 3.0 µl drop of chitosan solution and naturally dried up at room temperature. The modified working surface was then fixed with a 10µl drop of 0.1 M NaOH for 30 min and left it dried again prior to use.

2.3 Nucleic Acid Extraction

The phytoplasma DNA from diseased SCWL, BGWL and SP, each was extracted following the CTAB-phenol-chloroform method [13] from midrib of the leaves, the plant sieve elements where most phytoplasma cells are colonized [11]. The extracted DNA was purified by repeating this procedure again to get at least the purity index of 1.8 at A260/A280 ratio for a suitable direct use in the immobilization and hybridization trials. Its concentration was then quantified spectrophotometrically from the value measured at A260. The Challenging target nucleic acid from healthy plants was also extracted from midrib of the leaves by similar method. Stock solution of each nucleic acid sample was maintained in 10 mM Tris HCL pH 8.0 containing 1 mM Sodium EDTA (TE buffer) and kept frozen. The ssDNA was achieved by denaturing its native dsDNA in 100˚C water bath for 10 min and followed by rapid cooling in ice bath. This type of ssDNA was also prompted for subsequently used as probe to its complementary DNA hybridization.

2.4 Immobilization of DNA

The chitosan modified SPCE surface was employed as working platform for every challenging DNA immobilization experiments. Each DNA sample was immobilized by dropping 2 µl of its 10 µM inTE buffer onto the chitosan-modified SPCE platform and allowed to incubate overnight at room temperature. This functionalized surface was rinsed with 0.1% SDS phosphate buffer (pH 7.0) three times to remove the unbound DNA and dried at room temperature prior for the next manipulation.

2.5 DNA Hybridization

Hybridization, a reaction that is commonly recommended as an indication for specific recognition of the complementary DNA strand was due in this investigation. The reaction was performed by overspreading the ssDNA probe-functionalized spot surface of chitosan modified SPCE with a 3 µl droplet of 2 × SSC solvent containing 10 ng/µl challenging target ssDNA and kept incubating at 42˚C for 40 min. Afterward it was rinsed three times with 0.1% SDS phosphate buffer (pH 7.0). The testing hybridization performance was then ready for inspection after a minute of natural drying in air at room temperature.

2.6 AFM imaging and Analysis

A nanoscale imaging for the DNA immobilization and progressive hybridization event was carried out by an atomic force microscope model XE-70 (Park Systems Corp., Suwon, Korea) through a true non-contact mode. The observation was done under ambient conditions with standard PPP-NCHR silicon cantilever consisting of a < 10 nm tip radius (Nanosensors TM, Neuchâtel, Switzerland) with a spring constant of 42 N/m force constant and resonant frequency of 320 kHz. An x-y accessible 1×1up to 5×5 µm area with a Z scanner at 0.5 Hz scan rate was inspected with XEP software for data acquisition and XEI software for image processing and quantitative analysis of the surface topography. Relevant parameters such as line profile, an average roughness *Ra* (nm), standard deviation of the height value *Rq* (nm), skewness (*Rsk*), kurtosis (*Sku*), power spectrum density (PSD) algorithm, and fractal dimension were then successively identified.

3. RESULTS AND DISCUSSION

3.1 AFM Image and Characterization of The Dsdna and Ssdna Immobilized on Chitosan Modified Spce

A striking atomic force microscopy image of the intact double-stranded DNA (dsDNA) and its correlative two Single-stranded DNA (ssDNA) during the DNA strand separation consequence is perfectly manifested in Fig.1. This picture, in the meantime, declares a fiduciary distinguishing feature between the dsDNA and ssDNA molecules. Observation in all cases of the phytoplasma DNA from SCWL, BGWL and SP similarly and consistently presented the duplex dsDNA and ssDNA profiles as well (data not shown). In general, differentiation in UV light absorption measurement is the only technique for notifying the separation of the DNA strands [14]. The attained AFM image could thus be considered as the first direct visual evidence revealing a DNA separating posture simultaneously after the common denaturation process by heating. An important prerequisite one for this successful imaging is on account of a steady immobilization strategy. In our investigation, a DNA containing TE buffer droplet was simply deposited on the working surface of chitosan modified SPCE which adequately allowed stable and good quality AFM image without any complicate treatment.

It is indeed due to an excellent affinity of the natural chitosan polymer consisting of polycation function compatible for biological molecules including proteins, enzymes and DNA [1]-[5], [7], [8]. This multiple cation site chitosan matrix has been proved highly effective for immobilization of the DNA molecule in our previous experiments [1], [2], [5]. Its electrochemical capability has also been subsequently approved [7]. Affirmation on the DNA incident on the platform surface was proceed by the line analysis of AFM image using power spectral density (PSD) function of the waveguide algorithm. The PSD outcome is as illustrated in Fig. 2 that the density peak size of each DNA strand type could be obviously differentiated, the biggest PSD wave from dsDNA and the smaller two PSD waves from the other two ssDNA.

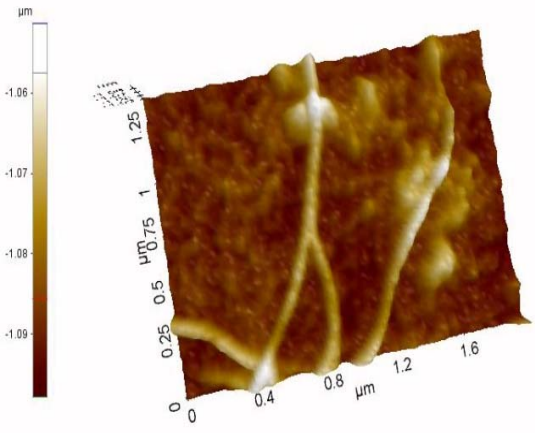

Fig.1 Three-dimensional AFM image at 1×1 µm scan size revealing surface morphology of dsDNA and the two ssDNA strands splitting from the dsDNA.

3.2 AFM Image Revealing the Conformation of Complementary DNA Strands upon Hybridization

The hybridization scheme was performed on chitosan modified SPCE working surface as summarized in Fig.3. This schematic presentation represents a generous process gained from SCWL, BGWL and SP phytoplasma genomic DNA. The ssDNA recognition probe was firmly immobilized on chitosan matrix surface of the electrode and subsequently hybridized with its complementary ssDNA target to form complete dsDNA molecule that can be detected simultaneously by an appropriate read-out systems such as the electrochemical voltammetry and the AFM in our cases [1], [2], [5], [7], [9].

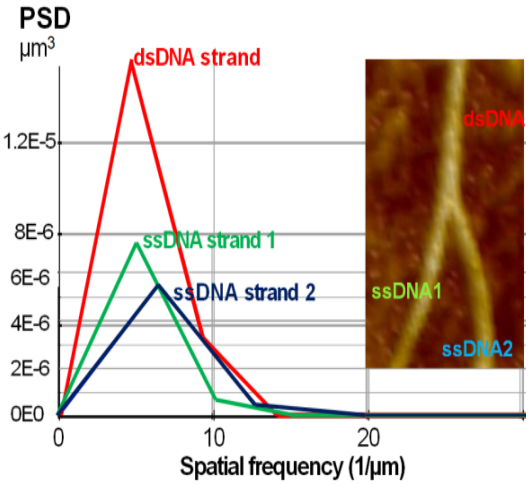

Fig. 2 Power spectral density (PSD) function of the waveguide analyzed along a line in the AFM image of dsDNA and the two ssDNA strands splitting from the dsDNA at 1×1 µmscan size.

By means of the non contact mode AFM observation, the hybridization incidence was directly visualized showing the duplex helical DNA tile forming clearly (Fig. 4). Their entangled appearance was ascertained by PSD analysis outcome expressing in Fig. 5. This AFM image indicates a dynamic of DNA hybridization since the beginning of the well-known Watson-Crick double helix state. The two complementary nucleotide strands were being tie to each other like a two ply rope with a right hand twisting. Herein, to our knowledge this captured image should also be the first direct visible double helix structure forming during the DNA hybridization. Successful direct imaging of the DNA hybridization in this simple technique was obtained by no harm or any damage to the DNA specimen which probably due to an excellent bioaffinity and protective effect of chitosan scaffold. Acceleration in DNA hybridization rate by two orders through facilitation of a nucleation step; a major rate determining step of hybridization was previously demonstrated in cationic polymer such as poly (L-lysine)-graft-dextran copolymer employing fluorescence-based assay [15]. The multiple cationic nature of chitosan polymer was therefore assumed to be an important factor accelerating the DNA hybridization which was found almost complete within 45 min in our observation. Meanwhile the combination trials of phytoplasma ssDNA with ssDNA from their healthy sugarcane,

burmuda grass and sesame plants yielded no sign of couple pairing or tying frame, hence referring to a mismatching nature of these non complementary strands.

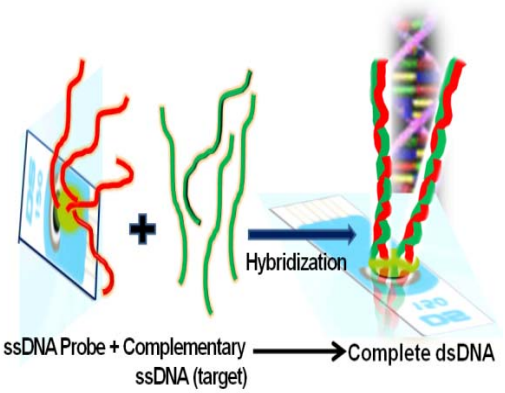

Fig.3 Schematic representation of the hybridization event on chitosan modified SPCE working surface for ssDNA probe (red) immobilization and subsequent hybridization with the complementary ssDNA target (green) to form a complete dsDNA as a result.

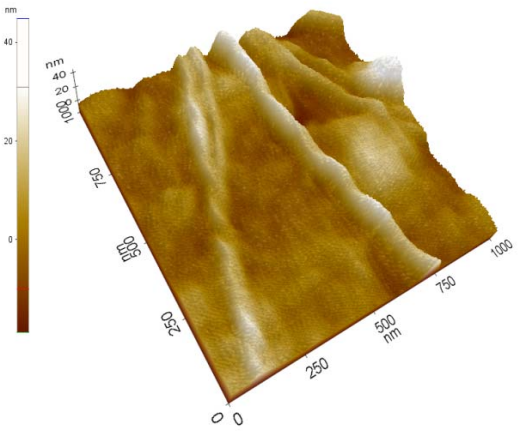

Fig.4 The tying complementary ssDNA strands into two-ply strand of the renowned double helix DNA captured image by AFM at 1×1 µm scan size.

3.3 AFM Surface Parameters Concerning the DNA Morphological Configuration

To determine the morphological configuration of the DNA, measurements based on the line analysis on surface topography of the AFM image was carried out using an XEI's Park System software. Interpretation of the measured data was

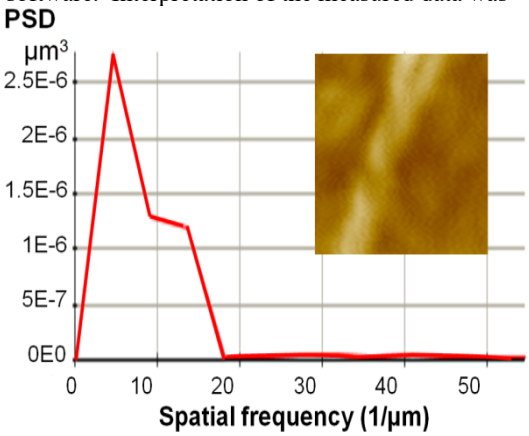

Fig.5 Power spectral density (PSD) profile from analyzed waveguide of the being hybridized DNA image at 1×1 µm scan size AFM investigation.

performed with reference to our previous reports [7], [8]. Important amplitude features were resolved by relevant statistical parameters that informed statistical average values and their standard deviation with a 0.05 significant level from 9 samples in total of each 3 replicates of the SCWL, BGWL and SP phytoplasma DNA cases as shown in Table 1. The DNA statures appeared in AFM images were estimated by their Δx, Δy and °A values from different cross sections lines to announce a differentiation between the dsDNA and ssDNA including the tying hybrid ssDNA pair. Regarding to the value 121.2 × 9.33 × 27.7 of dsDNA, 87.6 × 6.4 × 16.56 of ssDNA and 112.67 × 11.19 × 28.74 of the hybridized DNA measured by the Δx × Δy × °A, these values were remarkably 1.4 to 1.75 fold higher in dsDNA and the hybridized DNA than that of the ssDNA. The PSD values gained from dsDNA and hybridized DNA were also higher in peak volume by 2 to 3 folds. Therefore the form of double stranded DNA is apparently bigger than ssDNA by at least 1.4 orders. In general, an increase in fractal dimension value indicates a larger coverage of object. The fractal dimension parameter values obtained as 2.37 of the dsDNA and 2.47 of the hybridized DNA were thus explicit their bigger size in comparison to 2.26 of the ssDNA. On the other hand, the fractal dimension values on the surface between 2 and 3 are the values suggesting a top up aggregation of deposit molecule following a three dimension diffusion limited model [16] and our result is well agreed to this assumption. In the course of roughness profiles in terms of Ra and Rq parameters, values gained from the dsDNA and the hybrid DNA immobilized surfaces were about 1.34 to 1.73 folds rougher than the ssDNA. Two more

parameters, the roughness skewness (Rsk) and roughness kurtosis (Rku) were employed to measure a texture at the hill top of DNA statures in comparison to overall immobilized platform surface. A negative Rsk acquired in the hill top cases represents a good bearing platykurtoic surface of the DNA while a more negative value from the whole platforms indicates dominant valley surface underneath the DNA tile. The Rku values at the DNA hill top cases were all less than 3.00 which imply for a gradually varying feature of the surface. Whereas the values over than 3.00 were from Rku of the whole immobilized platform and thus explicate an evidence of a high DNA hill laid over the basal surfaces.

Table 1 Surface profile analyzed from AFM nanographs of the dsDNA, ssDNA and completely hybridized DNA at 1x1 μm scan size on chitosan modified SPCE platform.

Parameters	Ds DNA	ssDNA	Hybridized DNA
Δx (nm)	121.2 ± 11.96	87.6 ± 11.93	112.67 ± 6.43
Δy (nm)	9.33 ± 2.08	6.4 ± 2.41	11.19 ± 2.45
°A	27.7 ± 3.23	16.56 ± 1.02	28.74 ± 0.72
PSD (nm^3) 1	0.033 ± 0.01	0.01 ±0.001	0.007 ± 0.001
2	-	-	0.015 ± 0.008
Fractal dimension	2.37 ± 0.12	2.26 ± 0.05	2.47 ±0.06
Ra (nm)	9.11 ± 1.3	5.26 ± 0.14	7.74 ±0.04
Rq (nm)	9.92 ± 1.26	6.71 ± 0.17	8.96 ±0.86
Rsk hill surface	-0.39 ± 0.15	-0.75 ± 0.085	-0.77 ± 0.06
Rsk whole surface	-0.88 ± 0.15	-0.94 ± 0.62	-1.05 ± 0.09
Rku hill surface	2.21 ± 0.05	2.06 ± 0.042	2.24 ± 0.13
Rku whole surface	3.48 ± 0.05	3.28 ± 0.3	3.99 ±0.04

Note: °A = angle degree of a hill slope, Δx = horizontal distance Δy = vertical distance, PSD = power spectral density, *Ra* = roughness average, *Rq*= root mean square roughness, *Rsk* = skewness, Rku = kurtosis.

The results in this direct visual observation substantiate a success on steady immobilization and subsequent progressive hybridization of the long chain genomic DNA along with their measurable geographical characteristics. The non contact mode AFM has delivered considerably excellent resolution showing both the distinction between two types of DNA strands and the dynamic of complementary hybridization event. Although a bit limitation on an exact assessment was existed owning to the confine performance of a 10 nm radius standard AFM tip available at present-day which probably make inevitable over estimate in the DNA width that has been formerly reported to be about 2 nm according to crystallographic X-ray diffraction analysis [17]. More sophisticate AFM techniques were suggested for better scaling of DNA configuration such as the miniaturization of AFM cantilevers [18]; the use of frequency modulation AFM [19] and the use of peak force tapping mode including a typical tapping mode [20]. These techniques were found suitably operated with DNA aqueous solution samples. However the procedure of direct non contact mode AFM imaging in air is generally preferred still due to its simplicity and non-invasiveness, improvement concerning the non contact mode hardware including appropriate cantilever and its software combination is thus necessary. Notwithstanding the confinement of a simplest AFM model used in our investigation, a virtual image of the DNA and its differentiation is clearly demonstrated and sufficiently verified a real hybridization event empowering the effective of DNA biosensor performance.

4. CONCLUSIONS

The present work shows the first image capturing a striking posture of dsDNA separation and hybridization dynamic through a common non-contact mode AFM observation. A well known double helix forming state between two complementary ssDNA strands could be seen directly following hybridization process. All the trials with SCWL, BGWL and SP phytoplasma genomic DNA yielded similar performance from a very simple immobilization protocol employing the self assembled mechanism of the DNA containing 3 μl droplet onto chitosan modified SPCE basal surface. This successful direct imaging of the DNA dynamics was simply obtained in air at room temperature without any deteriorate effects to the observing DNA.

The apparent size of dsDNA and hybridized one seemed to be almost 2 folds wider than ssDNA. Their aggregation and growth mechanism on the basal platform surface were mainly directed vertically beyond a diffusion limited model

according to the line analysis results. By virtue of this finding, the reality of DNA immobilization and hybridization occurring event empowering an efficacy of the DNA biosensor can easily be verified and encouraged further development of real practicable diagnostic devices.

5. ACKNOWLEDGMENTS

The authors gratefully acknowledge Khon Kaen University's Division of Research and Technology Transfer Affair for partial funding and the KKU Research Instrument Center for instrumental facilitation. We also thank Mr. Supatr Chuaymee, Mr. Vorrayuth Mekarkat and Mr. Adirek Nakyan for their AFM technical assistances.

6. REFERENCES

[1] Wongkaew P., and Poosittisak S., Direct electrochemical DNA sensor for sugarcane white leaf disease diagnosis using label free DNA probes and oligochitosan self assembled monolayer-modified glassy carbon electrodes, in Proc. 2nd Int. Conf. on Technology and Innovation for Sustainable Development, 2008, pp. 504-507.

[2] Wongkaew P., and Poosittisak S., Diagnosis of sugarcane white leaf disease using the highly sensitive DNA based voltammetric electrochemical determination. Amer. J. of Plant Sciences, Vol. **5**, Issue 4, 2014, pp. 2256-2268.

[3] Sunon P., Wongkaew P., Johns J., and Johns N., Characterization of cerium oxide-chitosan nanocomposite-modified screen printed carbon electrode and application in melatonin determination. International Journal of GEOMATE, Vol. 14, Issue 42, 2018, pp.151-157.

[4] Wongkaew P., Wongkaew B., Saepaisan S., and Thanutong Pa., Development of specific electrochemical biosensor based on chitosan modified screen printed carbon electrode for the monitoring of captan fungicide. International Journal of GEOMATE, Vol. 14, Issue 43, 2018, pp. 55-62.

[5] Wongkaew P., and Poosittisak S., Electro-affinity of SCWL-dsDNA on different high deacetylation degree chitosans deposited glassy carbon electrode, Advances in Developing Affordable In-Vitro Molecular Diagnostics, Puri C.P., Abidi N., Bhanushali, P., Pere A., Gupta S.K., Eds., Mumbai: Yashraj Research Foundation, 2012, pp. 249-258.

[6] Sliwak A., Diez N., EwaMiniach E., and Gryglewicz G., Nitrogen-containing chitosan-based carbon as an electrode material for high-performance supercapacitors. Journal of Applied Eletrochemistry, Vol. 46, Issue 6, 2016, pp. 667-677.

[7] Wongkaew P., and Poosittisak S., Atomic force microscopic and electrochemical characterization of the modified screen printed carbon electrode by self assembled deposition of chitosan and activated carbon. International Journal of GEOMATE, Vol. 11, Issue 24, 2016, pp. 2356-2362.

[8] Wongkaew B, Wongkaew P., Thanutong Pa., and Thanutong C., Nanostructural characterization of glutathione-s-transferase immobilizing chitosan modified screen printed carbon electrode by atomic force microscopy. International Journal of GEOMATE, Vol. 14, Issue 43, 2018, pp. 132-139.

[9] Wongkaew **P.,** Sugarcane white leaf disease characterization, diagnosis development, and control strategies. Functional Plant Science Biotechnology, Vol. 6 (Special Issue 2, Sugarcane Pathology), 2012, pp. 73-84.

[10] Watson J.D. and Crick F.H., Molecular structure of nucleic acids: A structure for deoxyribose nucleic acid. Nature, Vol. 171, Issue 4356, 1953, pp. 737–738.

[11] Wongkaew P., Plant diseases caused by phytoplasma. Biosensing Technology for Sustainable Development Research Group's book publishing, Khon Kaen University, 2013, pp. 1-235.

[12] Variola F., Atomic force microscopy in biomaterials surface science. Phys. Chem. Chem. Physics, Vol. 17, Issue 5, 2015, pp. 2950-2959.

[13] Kollar A., Seemuller E., Bonnet F., Saillard C. and Bove J.M. Isolation of the DNA of Various Plant Pathogenic Mycoplasmalike Organisms from Infected Plants. Phytopathology,Vol. 80, No. 3, 1990, pp. 233-237.

[14] Ackerman M.M., Ricciardi C., Weiss D., Chant A., and Kraemer-Chant C.M., Analyzing Exonuclease-Induced Hyperchromicity by UV Spectroscopy: An Undergraduate Biochemistry Laboratory Experiment. Journal of Chemical Education, Vol. 93, Issue 12, 2016, pp. 2089-2095.

[15] Wu L, Shimada N, Kano A, Maruyama A, "Poly (L-lysine)-graft-dextran copolymer accelerates DNA hybridization by two orders", Soft Matter, Vol. 4, Issue 2, 2008, pp. 744–747.

[16] Ţălu S., Stach S., Ikram M., Pathak D., Wagner T., and Nunzi J-M., Surface roughness characterization of ZnO: TiO2-organic blended solar cells layers by atomic force microscopy and fractal analysis. Int. J Nanoscience, Vol. 13, No. 03, 2014, 12 pp.

[17] Fuller W., Wilkins W. H. F., Wilson H. R., and Hamilton L. D., The molecular configuration of deoxyribonucleic acid: IV. X-ray diffraction study of the A form. Journal of Molecular Biology, Vol. 12, Issue 1, 1965, pp. 60-76.

[18] Leung C., Bestembayeva A.,Thorogate R., Stinson J., Pyne A., Marcovich C., Yang J., Drechsler U., Despont M., Jankowski T., Tschöpe M., Bart W., and Hoogenboom B.W., Atomic force microscopy with nanoscale cantilevers resolves different structural conformations of the DNA double helix, Nano Letter, Vol.12, Issue 7,2012, pp. 3846−3850.

[19] Ido S., Kimura K., Oyabu N., Kobayashi K., Tsukada M., Matsushige K., and Yamada H., Beyond the helix pitch: direct visualization of native DNA in aqueous solution. ACS nano. Vol. 7, No. 2, 2013, pp. 1817–1822.

[20] PyneA.,Thompson R., Leung C , Roy D., and Hoogenboom B.W., Single-molecule reconstruction of oligonucleotide secondary structure by atomic force microscopy. Small, Vol. 10, Issue 16, 2014, pp. 3257–3261.